Neutrinophilic two Higgs doublet model with U(1) global symmetry

Kingman Cheung,^{1,2,3,*} Hiroshi Okada,^{1,†} and Yuta Orikasa^{4,‡}

¹Physics Division, National Center for Theoretical Sciences, Hsinchu, Taiwan 300

²Department of Physics, National Tsing Hua University, Hsinchu 300, Taiwan

³Division of Quantum Phases and Devices, School of Physics,

Konkuk University, Seoul 143-701, Republic of Korea

⁴Institute of Experimental and Applied Physics,

Czech Technical University, Prague 12800, Czech Republic

(Dated: September 15, 2021)

Abstract

We propose a neutrinophilic two-Higgs-doublet model, where the vacuum expectation value (VEV) of the second Higgs doublet is only induced at one-loop level via several neutral fermions. Thus, the masses of active neutrinos arising from the Higgs doublets are naturally small via such a tiny VEV. We discuss various phenomenology of the model, including the neutrino masses and oscillations, bounds on non-unitarity, lepton-flavor violations, the oblique parameters, the muon anomalous magnetic moment, the GeV-scale sterile neutrino candidate arising from the tiny VEV, and collider signatures. We finally discuss the possibility of detecting the sterile neutrino suggested in the experiment of Future Circular Collider (FCC).

^{*}Electronic address: cheung@phys.nthu.edu.tw

[†]Electronic address: macokada3hiroshi@cts.nthu.edu.tw

[‡]Electronic address: Yuta.Orikasa@utef.cvut.cz

I. INTRODUCTION

Two-Higgs-doublet models (THDM) are regarded as the simplest extensions of the standard model (SM) by adding one more doublet Higgs field to the Higgs sector [1]. It is the most often studied model because of its rich phenomenology and accommodation of the Higgs sector of supersymmetric models. Nevertheless, THDM's do not have enough matter contents to accommodate the small neutrino mass, at least in its simplest versions, conventionally dubbed as Types I, II, III, and IV.

Here we introduce an additional U(1) global symmetry with a set of exotic fermions and a singlet Higgs field, beyond the THDM. Among the exotic fermions, there are Dirac and Majorana types. The first Higgs doublet field Φ_1 is chosen to be the SM-like Higgs doublet while the second one Φ_2 to be inert at tree level. Yet, a tiny vacuum expectation value (VEV) is generated at loop level for the second doublet, which is then used to explain the small neutrino mass. Such a setup can explain the small neutrino mass without invoking extremely small Yukawa couplings.

In this work, in addition to showing that the model can explain neutrino mass and oscillation pattern, and non-unitarity bound, we also show that it can be consistent with existing limits on the lepton-flavor violations and the oblique parameters. Furthermore, we can have heavier sterile neutrinos of mass $\mathcal{O}(0.1 \sim 10)$ GeV, which are induced by the tiny VEV. Since the model also involves some exotic particles at TeV, we briefly describe the signatures that we can expect at the LHC.

This paper is organized as follows. In Sec. II, we describe the details of the model. In Sec. III, we study the phenomenology and constraints of the model, in particular, the derivations for the formulas of lepton-flavor violations, muon anomalous magnetic dipole moment (g-2), and the oblique parameters. In Sec. IV, we present the numerical analysis of the model. We conclude and discuss in Sec. V.

II. MODEL SETUP

In this section, we describe the neutrinophilic model in detail, including the bosonic sector, fermion sectors, and the scalar potential. First of all, we introduce an additional

	Fermions						Bosons		
Fermions	L_L	e_R	L'	N_{R_0}	N_1	N_{R_2}	Φ_1	Φ_2	φ
$SU(2)_L$	2	1	2	1	1	1	2	2	1
$U(1)_Y$	$-\frac{1}{2}$	-1	$-\frac{1}{2}$	0	0	0	$\frac{1}{2}$	$\frac{1}{2}$	0
U(1)	-1	-1	$-\frac{1}{5}$	0	$-\frac{1}{5}$	$-\frac{2}{5}$	0	3 5	$\frac{1}{5}$

TABLE I: Field contents of fermions and their charge assignments under $SU(2)_L \times U(1)_Y \times U(1)$, where each of the flavor index is abbreviated.

U(1) global symmetry. All the fermionic and bosonic contents and their assignments are summarized in Table I. Notice here that the numbers of family for all exotic fermions, except for N_{R_0} (two families), are three in order to reproduce the neutrino oscillation data, and L' and N_1 are Dirac-type fermions, while N_{R_0} and N_{R_2} are the Majorana fermions.

For the scalar sector with nonzero VEVs, we introduce two $SU(2)_L$ doublet scalars Φ_1 and Φ_2 , and an $SU(2)_L$ singlet scalar φ . Here Φ_1 is supposed to be the SM-like Higgs doublet, while Φ_2 is supposed to be an inert doublet at tree level. After spontaneous breaking of U(1) via φ , the VEV of Φ_2 is induced at the one-loop level via exotic fermions. Thus, a tiny VEV can theoretically be realized, which could be natural to generate the tiny neutrino masses.

In the framework of neutrinophilic THDM's, several scenarios have been considered in literature. For example, a tiny VEV is induced by bosonic loops at one-loop level with a global $U(1)_{B-L}$ symmetry and thus the active neutrinos are expected to be Dirac fermions [2]. The work in Ref. [3] had considered a tiny VEV generated at bosonic one-loop level with a $U(1)_R$ gauge symmetry, and all the light SM fermion masses are induced via this tiny VEV while the neutrino masses are induced at two-loop level as Majorana fermions. Another work in Ref [4] had considered the scenario in neutrinophilic THDM with a $U(1)_L$ global symmetry, in which neutrino masses are induced at tree-level as Majorana fermions and they also discussed the possibility of explaining the anomalous X-ray line. ¹

¹ In the framework of type-II seesaw models, there are also several models that a small $SU(2)_L$ triplet VEV can be induced at loop levels [5, 6].

A. Yukawa interactions and scalar sector

Yukawa Lagrangian: With the current field contents and symmetries, the renormalizable Lagrangian in the leptonic sector is given by

$$-\mathcal{L}_{L} = (y_{\ell})_{ii}\bar{L}_{L_{i}}\Phi_{1}e_{R_{i}} + f_{ij}\bar{L}'_{L_{i}}\tilde{\Phi}_{1}N_{R_{1j}} + f'_{ij}\bar{N}_{L_{i}}L'_{R_{j}}\Phi_{1} + g_{ij}\bar{L}'^{C}_{R_{i}}\Phi_{2}N_{R_{2j}} + (y_{L_{2}})_{ij}\bar{L}_{L_{i}}\tilde{\Phi}_{2}N_{R_{2j}}$$

$$+ (y_{N})_{ij}\bar{N}_{R_{2i}}N_{L_{1j}}\varphi + (y'_{N})_{ia}\bar{N}_{L_{1i}}N_{R_{0a}}\varphi + (y''_{N})_{ia}\bar{N}_{R_{1i}}N^{C}_{R_{0a}}\varphi + (M_{D})_{ij}\bar{N}_{L_{1i}}N_{R_{1j}}$$

$$+ (M_{0})_{aa}\bar{N}^{C}_{R_{0a}}N_{R_{0a}} + (M_{L'})_{ii}\bar{L}'_{L_{i}}L'_{R_{i}} + \text{c.c.},$$
(II.1)

where (i, j) = 1 - 3, a = 1, 2, $\tilde{\Phi}_{1,2} \equiv (i\sigma_2)\Phi_{1,2}^*$ with σ_2 being the second Pauli matrix, and the mass matrices in the last line are diagonal without loss of generality as well as y_{ℓ} .²

B. Fermion Sector

First of all, we define the exotic fermion as follows:

$$L'_{L(R)} \equiv \begin{bmatrix} N' \\ E'^{-} \end{bmatrix}_{L(R)}, \tag{II.2}$$

then the mass eigenvalue of charged fermion is straightforwardly given by $M_{L'}$ in Eq.(II.1). The mass matrix for the neutral exotic fermions is a 7×7 block in basis of $\Psi \equiv [\nu_L^C, N_{R_0}, N_{R_1}, N_{L_1}^C, N_{R_2}, N_R', N_L'^C]$, and given by

$$M_{N}(\Psi) = \begin{bmatrix} \mathbf{0}_{3\times3} & \mathbf{0}_{3\times2} & \mathbf{0}_{3\times3} & \mathbf{0}_{3\times3} & m_{D} & \mathbf{0}_{3\times3} & \mathbf{0}_{3\times3} \\ \mathbf{0}_{2\times3} & M_{0} & M_{N_{3}}^{T} & M_{N_{2}}^{T} & \mathbf{0}_{2\times3} & \mathbf{0}_{2\times3} \\ \mathbf{0}_{3\times3} & M_{N_{3}} & \mathbf{0}_{3\times3} & M_{D}^{T} & \mathbf{0}_{3\times3} & M^{T} \\ \mathbf{0}_{3\times3} & M_{N_{2}} & M_{D} & \mathbf{0}_{3\times3} & M_{N_{1}}^{T} & M' & \mathbf{0}_{3\times3} \\ m_{D}^{T} & \mathbf{0}_{3\times2} & \mathbf{0}_{3\times3} & M_{N_{1}} & \mathbf{0}_{3\times3} & m^{T} & \mathbf{0}_{3\times3} \\ \mathbf{0}_{3\times3} & \mathbf{0}_{3\times2} & \mathbf{0}_{3\times3} & M'^{T} & m & \mathbf{0}_{3\times3} & M_{L'} \\ \mathbf{0}_{3\times3} & \mathbf{0}_{3\times2} & M & \mathbf{0}_{3\times3} & \mathbf{0}_{3\times3} & M_{L'}^{T} & \mathbf{0}_{3\times3} \end{bmatrix},$$
(II.3)

where we define $m \equiv g_{ij}v_2/\sqrt{2}$, $m_D \equiv (y_{L_2})_{ij}v_2/\sqrt{2}$, $M \equiv f_{ij}v_1/\sqrt{2}$, $M' \equiv f'_{ij}v_1/\sqrt{2}$, $M_{N_1} \equiv (y_N)_{ij}v'/\sqrt{2}$, $M_{N_2} \equiv (y'_N)_{ia}v'/\sqrt{2}$, $M_{N_3} \equiv (y''_N)_{ia}v'/\sqrt{2}$. Then this matrix is diagonalized by a 20×20 unitary matrix V_N as $M_{\psi_\alpha} \equiv (V_N M_N V_N^T)_\alpha$ ($\alpha = 1 \sim 20$), where M_{ψ_α} consists of the mass eigenvalues.

² Although M_D is diagonal in general: $9 \to 3$; we select a symmetric M_D : $9 \to 6$; and reduced the parameter $y_{N'}$ by three degrees of freedom: $6 \to 3$. Thus the total degrees of freedom is conserved.

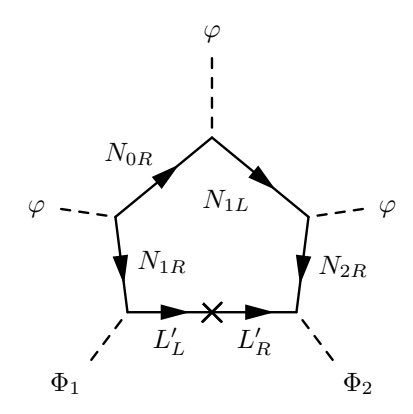


FIG. 1: 1 loop induced 5 dimensional operator

C. Scalar potential

In our model, the scalar potential is given by

$$V = \mu_{\varphi}^{2} |\varphi|^{2} + \lambda_{\varphi} |\varphi|^{4} + \sum_{i=1,2} \lambda_{\varphi\Phi_{i}} |\varphi|^{2} |\Phi_{i}|^{2}$$

$$+ \mu_{11}^{2} |\Phi_{1}|^{2} + \mu_{22}^{2} |\Phi_{2}|^{2} + \frac{\lambda_{1}}{2} |\Phi_{1}|^{4} + \frac{\lambda_{2}}{2} |\Phi_{2}|^{4} + \lambda_{3} |\Phi_{1}|^{2} |\Phi_{2}|^{2} + \lambda_{4} |\Phi_{1}^{\dagger}\Phi_{2}|^{2}, \qquad (II.4)$$

where we have chosen some parameters in the potential such that $\langle \Phi_2 \rangle \equiv v_2/\sqrt{2} = 0$ at tree level, while $\varphi = \frac{1}{\sqrt{2}}(v' + \varphi_R + iG)$ with $v' \neq 0$ and $\langle \Phi_1 \rangle \equiv v_1/\sqrt{2} \neq 0$. Here φ_R is assumed to be the mass eigenstate that suggests the mass of φ_R is larger than the other mass eigenvalues. G is the physical Goldstone boson (GB) that does not mix with other particles. To achieve the inert Φ_2 , we impose the inert conditions as follows:

$$0 < \lambda_2, \quad 0 \le 2\mu_{22}^2 + (\lambda_3 + \lambda_4)v_1^2 + \lambda_{\varphi\Phi_2}v'^2$$

A five-demensional operator $\lambda_5 \varphi^3 \Phi_2^{\dagger} \Phi_1$ can be generated at one-loop level as shown in Fig.1. The formula is given by

$$\lambda_{5} = \sum_{a=1}^{20} \frac{4M_{L'_{j}}}{(4\pi)^{2}} \left[f_{i,m} g_{i,j} (y_{N})_{j,k} (y_{N}')_{k,l} (y_{N}'')_{m,l} \right] F\left(4, 1, \{M_{0_{i}}^{2}, M_{L'_{j}}^{2}, M_{D_{k}}^{2}, M_{D_{l}}^{2}\}\right), \quad (II.5)$$

where the explicit expression for $F\left(4,1,\{M_{0_i},M_{L'_j},M_{D_k},M_{D_l}\}\right)$ is given in Appendix A. After the spontaneous symmetry breaking, an effective mass term $\mu_{12}^2\Phi_2^{\dagger}\Phi_1=\frac{\lambda_5 v'^3}{2\sqrt{2}}\Phi_2^{\dagger}\Phi_1$ is

obtained. The resultant scalar potential in the THDM Higgs sector is given by

$$V_{THDM} = \mu_{12}^2 (\Phi_1^{\dagger} \Phi_2 + \text{c.c.}) + \mu_{11}^{\prime 2} |\Phi_1|^2 + \mu_{22}^{\prime 2} |\Phi_2|^2 + \frac{\lambda_1}{2} |\Phi_1|^4 + \frac{\lambda_2}{2} |\Phi_2|^4 + \lambda_3 |\Phi_1|^2 |\Phi_2|^2 + \lambda_4 |\Phi_1^{\dagger} \Phi_2|^2,$$
 (II.6)

where $\mu_{11(22)}^{\prime 2} \equiv \mu_{11(22)}^2 + \lambda_{\varphi \Phi_{1(2)}} v'^2/2$, $\langle \Phi_i \rangle \equiv v_i/\sqrt{2} \ (i=1-2)$ and we choose μ_{12}^2 to be negative, while μ_{11}^2 to be positive, and assume that $v_2/v' \ll 1$. Taking $v_2/v_1 \ll 1$, we finally obtain the formula for the VEV of Φ_2 as

$$v_2 \approx \frac{2v_1\mu_{12}^2}{2\mu_{22}^{\prime 2} + v_1^2(\lambda_3 + \lambda_4)}. (II.7)$$

Including their VEVs, the scalar fields are parameterized as

$$\Phi_{1} = \begin{bmatrix} h_{1}^{+} \\ \frac{v_{1} + h_{1} + ia_{1}}{\sqrt{2}} \end{bmatrix}, \quad \Phi_{2} = \begin{bmatrix} h_{2}^{+} \\ \frac{v_{2} + h_{2} + ia_{2}}{\sqrt{2}} \end{bmatrix}.$$
 (II.8)

After the spontaneous symmetry breaking, the neutral scalar bosons φ_R and h_1 mix each other to form mass eigenstates. Note that the VEV of the second Higgs doublet is too small for a sizeable mixing with h_2 . The pseudoscalar components and the charged components are rotated to give the zero-mass Goldstone bosons and the physical pseudoscalar Higgs boson and charged Higgs boson, respectively. They are given in the following expressions:

$$\begin{aligned} \text{Diag.}(m_{H_1^0}^2, m_{H_2^0}^2) &= O_H m^2(\varphi_R, h_1) O_H^T, \\ \text{Diag.}(m_{Z^0}^2, m_{A^0}^2) &= O_I m^2(a_1, a_2) O_I^T, \\ \text{Diag.}(m_{\omega^{\pm}}^2, m_{H^{\pm}}^2) &= O_C m^2(h_1^{\pm}, h_2^{\pm}) O_C^T, \end{aligned}$$
(II.9)

where $O_{H,C,I}$ denotes the mixing matrices which diagonalize the mass matrices accordingly. Here Z^0 and ω^{\pm} are zero-mass Goldstone bosons to be absorbed as the longitudinal component of the neutral SM gauge boson Z and charged gauge boson W^{\pm} respectively. The mass matrices in the right-hand side of Eq. (II.9) are given by the parameters in the scalar potential. For neutral CP-even components we obtain

$$m^{2}(\varphi_{R}, h_{1}) \sim \begin{bmatrix} 2\lambda_{\varphi}v'^{2} & v_{1}v'\lambda_{\varphi\Phi_{1}} \\ v_{1}v'\lambda_{\varphi\Phi_{1}} & 2\lambda_{1}v_{1}^{2} - \frac{v_{2}\mu_{12}^{2}}{v_{1}} \end{bmatrix},$$
 (II.10)

where $H_1^0(\equiv h_{SM})$ is the SM-like Higgs in our notation, and h_2 does not mix in the limit of $\mu_{12}, v_2 \ll v_1, v_{\varphi}; m_{h_2}^2 \sim 2\lambda_2 v_2^2 - \frac{v_2 \mu_{12}^2}{v_2}$. We also obtain the mass matrices for CP-odd and

charged components as

$$m^{2}(a_{1}, a_{2}) = \begin{bmatrix} -\frac{v_{2}\mu_{12}^{2}}{v_{1}} & \mu_{12}^{2} \\ \mu_{12}^{2} & -\frac{v_{1}\mu_{12}^{2}}{v_{2}} \end{bmatrix}, \quad m_{A^{0}}^{2} = -\frac{(v_{1}^{2} + v_{2}^{2})\mu_{12}^{2}}{v_{1}v_{2}},$$

$$m^{2}(h_{1}^{\pm}, h_{2}^{\pm}) = \begin{bmatrix} -\frac{v_{2}(\lambda_{4}v_{1}v_{2} + 2\mu_{12}^{2})}{2v_{1}} & \frac{\lambda_{4}v_{1}v_{2}}{2} + \mu_{12}^{2} \\ \frac{\lambda_{4}v_{1}v_{2}}{2} + \mu_{12}^{2} & -\frac{v_{1}(\lambda_{4}v_{1}v_{2} + 2\mu_{12}^{2})}{2v_{2}} \end{bmatrix}, \quad m_{H^{\pm}}^{2} = -\frac{(v_{1}^{2} + v_{2}^{2})(\lambda_{4}v_{1}v_{2} + 2\mu_{12}^{2})}{2v_{1}v_{2}}.$$
(II.12)

Here we explicitly show the 2×2 matrices; O_R, O_C, O_I , as

$$O_R \equiv \begin{bmatrix} c_{\alpha} & s_{\alpha} \\ -s_{\alpha} & c_{\alpha} \end{bmatrix}, \qquad O_I \equiv O_C = \begin{bmatrix} c_{\beta} & s_{\beta} \\ -s_{\beta} & c_{\beta} \end{bmatrix}, \quad s_{\beta} = \frac{v_2}{\sqrt{v_1^2 + v_2^2}}, \tag{II.13}$$

where $c_{\alpha(\beta)} \equiv \cos \alpha(\beta)$ and $s_{\alpha}(\beta) \equiv \sin \alpha(\beta)$, and we define $v \equiv \sqrt{v_1^2 + v_2^2}$, $\tan \beta \equiv \frac{v_2}{v_1}$ which lead $v_1 = v \cos \beta$ and $v_2 = v \sin \beta$ as in the other THDMs. Since $v_2 \ll v_1$ is achieved theoretically, $s_{\beta} \ll 1$ is realized. Also s_{α} is written in terms of the elements of $m^2(\varphi_R, h_1)$, which is restricted by the current experimental data at LHC $s_{\alpha} \lesssim 0.3$. Note that there is an advantage of introducing fermions inside the loop instead of bosons [2, 3], because of the positivity of the fermion-loop contributions to the pure quartic couplings. Hence the vacuum stability can easily be realized [7].

III. PHENOMENOLOGY AND CONSTRAINTS

A. Neutrino masses and Oscillations

The charged-lepton mass is given by $m_{\ell} = y_{\ell}v/\sqrt{2}$ after the electroweak symmetry breaking, where m_{ℓ} is assumed to be the mass eigenstate. Let us redefine the neutral mass matrix M_N , its mixing matrix V_N and mass eigenvalues M_{ψ} as two by two block-mass matrices for the convenience of discussing the non-unitarity of leptonic mixing matrix [8]:

$$M_N = \begin{bmatrix} 0_{3\times3} & m_{3\times17} \\ m_{17\times3}^T & M_{17\times17} \end{bmatrix}, \quad M_{\psi} = \begin{bmatrix} d_{3\times3} & 0_{3\times17} \\ 0_{17\times3}^T & D_{17\times17} \end{bmatrix}, \quad (\text{III.1})$$

$$V_N = \begin{bmatrix} (V_N)_{3\times3} & 0_{3\times17} \\ 0_{17\times3}^T & (V_N)_{17\times17} \end{bmatrix} \begin{bmatrix} 1_{3\times3} & X_{3\times17}^{\dagger} \\ X_{17\times3} & 1_{17\times17} \end{bmatrix},$$
(III.2)

where $(V_N)_{3\times3}$ and $d_{3\times3}$ correspond, respectively, to the lepton-mixing matrix with non-unitarity, and mass eigenvalues of active neutrinos. With several steps, X can be parametrized by

$$X = \pm i\sqrt{D^{-1}}\mathcal{O}\sqrt{d},\tag{III.3}$$

where \mathcal{O} is an arbitrary 17×3 matrix with 45 degrees of freedom, satisfying $\mathcal{O}^T \mathcal{O} = 1_{3\times 3}$ but $\mathcal{O}\mathcal{O}^T \neq 1_{17\times 17}$. Next, consider the Hermitian matrix $X^{\dagger}X$ being diagonalized by a unitary 3×3 mixing matrix U, i.e., $d_X^2 \equiv U^{\dagger}X^{\dagger}XU$. Then the non-unitarity parameter η , which is defined by $(V_N)_{3\times 3} \equiv (1-\eta)V_{MNS}$, should be smaller than the following bounds that arise from global constraints in Ref. [9]

$$|2\eta| \simeq |V_k d_X^2 V_k^{\dagger}| \lesssim \begin{bmatrix} 2.5 \times 10^{-3} & 2.4 \times 10^{-5} & 2.7 \times 10^{-3} \\ 2.4 \times 10^{-5} & 4.0 \times 10^{-4} & 1.2 \times 10^{-3} \\ 2.7 \times 10^{-3} & 1.2 \times 10^{-3} & 5.6 \times 10^{-3} \end{bmatrix},$$
(III.4)

$$V_{MNS} = \begin{bmatrix} c_{13}c_{12} & c_{13}s_{12} & s_{13}e^{-i\delta} \\ -c_{23}s_{12} - s_{23}s_{13}c_{12}e^{i\delta} & c_{23}c_{12} - s_{23}s_{13}s_{12}e^{i\delta} & s_{23}c_{13} \\ s_{23}s_{12} - c_{23}s_{13}c_{12}e^{i\delta} & -s_{23}c_{12} - c_{23}s_{13}s_{12}e^{i\delta} & c_{23}c_{13} \end{bmatrix} \begin{bmatrix} e^{i\alpha_{1}/2} & 0 & 0 \\ 0 & e^{i\alpha_{2}/2} & 0 \\ 0 & 0 & 1 \end{bmatrix},$$
(III.5)

where V_{MNS} is the unitary 3×3 lepton-mixing matrix that is observed, and $V_k \equiv (V_N)_{3\times 3}U_{3\times 3}(\sqrt{1+d_X^2})_{3\times 3}$. In our numerical analysis, we implicitly satisfy this condition.

In addition to the bounds on non-unitarity, we further impose the following ranges on

$$V_{MNS}^{\dagger}dV_{MNS}^{*} = \begin{bmatrix} 0.0845 - 0.475 & 0.0629 - 0.971 & 0.0411 - 0.964 \\ 1.44 - 3.49 & 1.94 - 2.85 \\ * & 1.22 - 3.33 \end{bmatrix} \times 10^{-11} \text{ GeV}, \quad \text{(III.6)}$$

where we have used the following neutrino oscillation data at 3σ [10] in case of normal

³ This can easily be satisfied by controlling 45 free parameters of \mathcal{O} .

Process	(i,j)	Experimental bounds (90% CL)	References
$\mu^- \to e^- \gamma$	(2,1)	$BR(\mu \to e\gamma) < 4.2 \times 10^{-13}$	[11]
$\tau^- \to e^- \gamma$	(3,1)	$Br(\tau \to e\gamma) < 3.3 \times 10^{-8}$	[12]
$\tau^- \to \mu^- \gamma$	(3, 2)	$BR(\tau \to \mu \gamma) < 4.4 \times 10^{-8}$	[12]

TABLE II: Summary of $\ell_i \to \ell_j \gamma$ process and the lower bound of experimental data.

hierarchy (NH) given by ⁴

$$0.278 \le s_{12}^2 \le 0.375, \ 0.392 \le s_{23}^2 \le 0.643, \ 0.0177 \le s_{13}^2 \le 0.0294, \ \delta \in [-\pi, \pi],$$

$$\sqrt{m_{\nu_3}^2 - \frac{m_{\nu_1}^2 + m_{\nu_2}^2}{2}} = (\sqrt{23.0} - \sqrt{26.5}) \times 10^{-11} \text{ GeV},$$

$$\sqrt{m_{\nu_2}^2 - m_{\nu_1}^2} = (\sqrt{0.711} - \sqrt{0.818}) \times 10^{-11} \text{ GeV},$$
(III.8)

and the Majorana phases $\alpha_{1,2}$ taken to be $\alpha_{1,2} \in [-\pi, \pi]$.

In case of inverted hierarchy (IH) we also impose the following ranges at 3σ confidential level [10]:

$$V_{MNS}^{\dagger}dV_{MNS}^{*} = \begin{bmatrix} 1.00 - 5.00 & 0.00237 - 3.83 & 0.00256 - 3.94 \\ * & 0.00279 - 3.08 & 0.365 - 2.60 \\ * & * & 0.00500 - 3.30 \end{bmatrix} \times 10^{-11} \text{ GeV}, \quad \text{(III.9)}$$

$$0.403 \le s_{23}^{2} \le 0.640, \ 0.0183 \le s_{13}^{2} \le 0.0297,$$

$$\sqrt{\frac{m_{\nu_{1}}^{2} + m_{\nu_{2}}^{2}}{2} - m_{\nu_{3}}^{2}} = (\sqrt{22.0} - \sqrt{25.4}) \times 10^{-11} \text{ GeV}, \quad \text{(III.10)}$$

where the other values are same as the case of NH.

B. Sterile neutrino

Due to two of the blocks in the mass matrix for neutral fermions, m and m_D , in Eq. (II.3), we can have another three lighter neutral fermions in addition to the three active neutrinos. Hence the model can provide GeV-scale sterile neutrino(s) that have been studied in the

⁴ Recently $\delta = -\pi/2$ is experimentally favored. But our result does not change significantly, even if we fix $\delta = -\pi/2$.

Future Circular Collider (FCC) proposal [22, 23]. Here let us focus on the lightest sterile fermion $\psi_4 \equiv \nu_s$, and its mass is defined by m_{ν_s} . Since the testability of FCC is provided in terms of m_{ν_s} and its mixing between ν_s and three active neutrinos [24], we define its mixing as follows:

$$\theta_s \equiv \sqrt{|V_{4,1}|^2 + |V_{4,2}|^2 + |V_{4,3}|^2},$$
(III.11)

where θ_s depends on each of mass values in Eq. (II.3). ⁵ The concrete analysis will be give in the next section.

C. Lepton Flavor Violations (LFVs)

First of all, we rewrite the leptonic interacting Lagrangian in terms of the mass eigenstates as follows:

$$-\mathcal{L}_{int}^{L} = -c_{\beta} \sum_{i,j=1}^{3} \sum_{a=1}^{20} (y_{L_2})_{i,j} V_{N_{j+11,a}}^{T} \bar{\ell}_{L_i} \psi_{R_a} H^- + \text{h.c.}.$$
 (III.12)

Then lepton-flavor violating processes $\ell_i \to \ell_j \gamma$ will give constraints on our parameters, where the experimental bounds are listed in Table. II. The branching ratio for $\ell_i \to \ell_j \gamma$ is given by

$$BR(\ell_i \to \ell_j \gamma) \approx \frac{48\pi^3 \alpha_{em} C_{ij} c_\beta^2}{G_F^2} \left| \sum_{k,k'=1}^3 \sum_{\alpha=1}^{20} \frac{(y_{L_2})_{j,k} V_{N_{k+11,\alpha}}^T (y_{L_2}^{\dagger})_{k',i} V_{N_{\alpha,k'+11}}^*}{(4\pi)^2} F_{lfv}(M_{\psi_{\alpha}}, m_{H^{\pm}}) \right|^2$$

$$\approx \frac{192\pi^3 \alpha_{em} C_{ij}}{(4\pi)^2 v_2^4 G_F^2} \left| \sum_{k,k'=1}^3 \sum_{\alpha=1}^{20} m_{D_{j,k}} V_{N_{k+11,\alpha}}^T m_{D_{k',i}}^\dagger V_{N_{\alpha,k'+11}}^* F_{lfv}(M_{\psi_\alpha}, m_{H^{\pm}}) \right|^2, \tag{III.13}$$

$$F_{lfv}(m_a, m_b) = \frac{2m_a^6 + 3m_a^4 m_b^2 - 6m_a^2 m_b^4 + m_b^6 + 12m_a^4 m_b^2 \ln(m_b/m_a)}{12(m_a^2 - m_b^2)^4},$$
 (III.14)

where $\alpha_{em} \approx 1/137$ is the fine-structure constant, $C_{ij} = (1, 0.178, 0.174)$ for $((i, j) = ((2, 1), (3, 2), (3, 1)), G_F \approx 1.17 \times 10^{-5} \text{ GeV}^{-2}$ is the Fermi constant.

⁵ One may consider the possibility of a (decaying) dark matter candidate with a lighter mass scale of keV or MeV, since single photon emission can be possible due to the mixing whose form is the same as the sterile one. However, since the typical mixing of our model at this mass scale is $0.01 \sim 0.0001$, which is too large to explain, e.g., x-ray line at 3.55 keV or 511 keV line, which requires a typical mixing $10^{-5} \sim 10^{-6}$. Thus, the only possibility to detect in experiments could be sterile neutrinos.

Muon anomalous magnetic dipole moment $(g-2)_{\mu}$: Through the same process as the above LFVs, there exists the contribution to $(g-2)_{\mu}$, and its form Δa_{μ} is simply given by

$$\Delta a_{\mu} \approx -\frac{m_{\mu}^{2} c_{\beta}^{2}}{(4\pi)^{2}} \left[\sum_{k,k'=1}^{3} \sum_{\alpha=1}^{20} (y_{L_{2}})_{2,k} V_{N_{k+11,\alpha}}^{T} (y_{L_{2}}^{\dagger})_{k',2} V_{N_{\alpha,k'+11}}^{*} \right] F_{lfv}(M_{\psi_{\alpha}}, m_{H^{\pm}})$$

$$\approx -\frac{2m_{\mu}^{2}}{(4\pi)^{2} v_{2}^{2}} \left[\sum_{k,k'=1}^{3} \sum_{\alpha=1}^{20} m_{D_{2,k}} V_{N_{k+11,\alpha}}^{T} m_{D_{k',2}}^{\dagger} V_{N_{\alpha,k'+11}}^{*} \right] F_{lfv}(M_{\psi_{\alpha}}, m_{H^{\pm}}). \quad (III.15)$$

Although this value can be tested by current experiments $\Delta a_{\mu} = (28.8 \pm 8.0) \times 10^{-10}$ [13], one cannot obtain a positive muon g-2 in the current model.

D. Oblique parameters

Since we have exotic fermions L' with $SU(2)_L$ doublet, we have to consider the oblique parameters that restrict the mass hierarchy between each of the components of multiple fermions. In our case, the masses between E' and ψ_a are restricted. The first task is to write down their kinetically interacting Lagrangians in terms of mass eigenstate, and they are give by

$$\mathcal{L} \sim \frac{g_2}{\sqrt{2}} \sum_{a=1}^{20} \left(V_{N_{a,\alpha+17}} \bar{\psi}_a \gamma^{\mu} P_L E'_{\alpha} W^+_{\mu} + V^*_{N_{a,\alpha+14}} \bar{\psi}_a \gamma^{\mu} P_R E'_{\alpha} W^+_{\mu} + \text{h.c.} \right) \qquad (III.16)$$

$$+ \frac{g_2}{2c_w} \sum_{a,b=1}^{20} \left[V_{N_{a,\alpha+17}} V^{\dagger}_{N_{\alpha+17,b}} \bar{\psi}_a \gamma^{\mu} P_L \psi_b + V^*_{N_{a,\alpha+14}} V^T_{N_{\alpha+14,b}} \bar{\psi}_a \gamma^{\mu} P_R \psi_b + \left(-1 + 2s_w^2 \right) \bar{E}'_{\alpha} \gamma^{\mu} E'_{\alpha} \right] Z_{\mu}, \tag{III.17}$$

Here we focus on the new physics contributions to ΔS and ΔT parameters in the case $\Delta U = 0$. Then ΔS and ΔT are defined as

$$\Delta S = 16\pi \frac{d}{dq^2} [\Pi_{33}(q^2) - \Pi_{3Q}(q^2)]|_{q^2 \to 0}, \quad \Delta T = \frac{16\pi}{s_W^2 m_Z^2} [\Pi_{\pm}(0) - \Pi_{33}(0)], \quad (III.18)$$

where $s_W^2 \approx 0.23$ is the Weinberg angle and m_Z is the Z boson mass, and $\Pi_{33(3Q)(\pm)}$ consists of the fermion-loop L' and boson loop Φ_2 . The fermion loop factors $\Pi_{33,3Q,\pm}^f(q^2)$ are calculated from the one-loop vacuum-polarization diagrams for Z and W^{\pm} bosons, which are

respectively given by

$$\Pi_{\pm}^{f}(q^{2}) = \frac{V_{\alpha+14,a}^{T}V_{\alpha,\alpha+14}^{*} + V_{N_{\alpha+17,a}}^{\dagger}V_{N_{a,\alpha+17}}}{(4\pi)^{2}} \int_{0}^{1} dx \ln \left[-x(1-x)\frac{q^{2}}{M_{E_{\alpha}'}^{2}} + x + (1-x)\frac{M_{\psi_{a}}^{2}}{M_{E_{\alpha}'}^{2}} \right] \\
\times \left[2x(1-x)q^{2} - xM_{E_{\alpha}'}^{2} - (1-x)M_{\psi_{a}}^{2} \right], \qquad (III.19) \\
\Pi_{33}^{f}(q^{2}) = \frac{1}{2(4\pi)^{2}} \int_{0}^{1} dx \left(\ln \left[-x(1-x)\frac{q^{2}}{M_{E_{\alpha}'}^{2}} + 1 \right] \left[2x(1-x)q^{2} - M_{E_{\alpha}'}^{2} \right] \right) \\
+ \left[(V_{N_{\alpha+14,a}}^{T}V_{N_{a,\beta+14}}^{*})(V_{N_{\beta+14,b}}^{T}V_{N_{b,\alpha+14}}^{*}) + (V_{N_{\alpha+17,a}}^{\dagger}V_{N_{a,\beta+17}})(V_{N_{\beta+17,b}}^{\dagger}V_{N_{b,\alpha+17}}) \right] \\
\times \ln \left[-x(1-x)\frac{q^{2}}{M_{\psi_{a}}^{2}} + x + (1-x)\frac{M_{\psi_{b}}^{2}}{M_{\psi_{a}}^{2}} \right] \left[2x(1-x)q^{2} - xM_{\psi_{a}}^{2} - (1-x)M_{\psi_{b}}^{2} \right], \qquad (III.21) \\
\Pi_{3Q}^{f}(q^{2}) = \frac{2}{(4\pi)^{2}} \int_{0}^{1} dx \ln \left[-x(1-x)\frac{q^{2}}{M_{E_{\alpha}'}^{2}} + 1 \right] \left[2x(1-x)q^{2} - M_{E_{\alpha}'}^{2} \right], \qquad (III.21)$$

where a(b) runs 1-20, while $\alpha(\beta)$ runs 1-3. While the boson case are directly given as ΔS^b and ΔT^b [14];

$$\Delta S^b \approx \frac{1}{2\pi} \int_0^1 dx x (1-x) \ln \left[\frac{x m_{h_2}^2 + (1-x) m_{A^0}^2}{m_{H^{\pm}}^2} \right], \tag{III.22}$$

$$\Delta T^b \approx \frac{1}{32\pi^2 v^2 \alpha_{em}} [F(m_{H^{\pm}}, m_{A^0}) + F(m_{H^{\pm}}, m_{h_2}) - F(m_{A^0}, m_{h_2})], \tag{III.23}$$

$$F(m_1, m_2) \equiv \frac{m_1^2 + m_2^2}{2} - \frac{m_1^2 m_2^2}{m_1^2 - m_2^2} \ln \frac{m_1^2}{m_2^2},$$
(III.24)

where we assume to be the no mixing among each of component Φ_2 . The experimental bounds are given by [15]

$$(0.07 - 0.08) \le \Delta S \le (0.07 + 0.08), \quad (0.10 - 0.07) \le \Delta T \le (0.10 + 0.07).$$
 (III.25)

In theoretical point of view, ΔT mainly corresponds to the mass differences between each of component inside the loop field, and $\Delta T = 0$ is obtained in the limit of $M_{E'} = M_{\Psi}$ as well as $m_{h_2} = m_{H^{\pm}}$ without loss of generality. While ΔS corresponds to the number of new fields, and more new fields give more deviations from $\Delta S = 0$. As another point of view, one can obtain opposite sign of contributions depending on the fermion loop or boson loop. For example, we always find positive value of ΔS^f . If the value of ΔS^f exceeds the experimental bound 0.15, we can decrease the value by controlling $m_{h_2} < m_{H^{\pm}}$ whose condition leads to negative value of ΔS^b . As a quantitative aspect, the absolute value of ΔS is always less than 1 in our framework, while the one of ΔT can fluctuate any value depending on the

mass differences. Hence fitting the ΔT could be non-trivial and tends to be difficult. In addition, considering that m_{h_2} can actually be considered as a free parameter and one can always be $\Delta S = 0$, we focus on ΔT .

E. Collider Signatures

1. Issue of the Goldstone Boson

Here we show the mechanism that can generate a nonzero mass for the Goldstone boson G. The mass is induced at higher order terms via gravitational effects that violate the global U(1) symmetry, and its relevant Lagrangian is given by [19] ⁶

$$-\delta \mathcal{L}_G \sim \lambda_5 \frac{\varphi^5}{M_{pl}} + \lambda_6 \frac{\varphi^4 \varphi^*}{M_{pl}} + \lambda_7 \frac{\varphi^3 \varphi^{*2}}{M_{pl}} + \text{c.c.}, \qquad (III.26)$$

where $M_{pl} \approx 1.22 \times 10^{19}$ GeV is the Planck mass. From this dimension-5 operator, one straightforwardly finds the following mass for G:

$$m_G \approx \frac{1}{5} \sqrt{\frac{25}{2} \lambda_5 + \frac{9}{2} \lambda_6 + \frac{1}{2} \lambda_7} \left[\frac{v'}{v_1} \right]^{3/2} \text{ keV},$$
 (III.27)

where $v_1 \ll v'$ is assumed. Here we suppose that the upper bound on m_G is $\mathcal{O}(1)$ MeV.

The Goldstone boson G has the following interactions after the $U(1)_L$ symmetry breaking[20, 21]:

$$\mathcal{L}_{eff} \supset \frac{1}{v'} (\partial_{\mu} G) (\bar{\ell} \gamma^{\mu} \ell + \bar{\nu} \gamma^{\mu} P_{L} \nu). \tag{III.28}$$

Thus, we have annihilation modes of active neutrino pairs via φ_R in the s-channel. This can be induced through the mixing among neutral fermions, and their interactions are found to be

$$-\mathcal{L}_{\varphi\psi\bar{\psi}} \sim \frac{\varphi_R + iG}{\sqrt{2}} \left[(y_N)_{ij} \bar{N}_{R_{2i}} N_{L_{1j}} + (y_N')_{kl} \bar{N}_{L_{1k}} N_{R_{0l}} + (y_N'')_{mn} \bar{N}_{R_{1m}} N_{R_{0n}}^C \right] + \text{h.c.}$$

$$= (\varphi_R + iG) \sum_{a,b=1}^{20} \left[(Y_L)^{ab} \bar{\psi}_a P_L \psi_b^C + (Y_R)^{ab} \bar{\psi}_a^C P_R \psi_b \right], \qquad (\text{III.29})$$

⁶ These interactions among G could affect invisible decays, cosmic string and so on. However since these constraints are very weak due to the vector-like current [16, 17], we do not need to worry about these issues. See also, *i.e.*, Ref. [18] for discussing phenomenologies of GB at collider physics.

where

$$(Y_L)^{ab} = \frac{1}{\sqrt{2}} \sum_{i,j=1}^{3} \left[V_{N_{a,i+11}}^*(y_N)_{i,j} V_{N_{j+8,b}}^T - V_{N_{a,i+8}}^*(y_N'^{\dagger})_{i,j} V_{N_{j+3,b}}^T + V_{N_{a,i+5}}^*(y_N'')_{i,j} V_{N_{j+3,b}}^T \right]$$

$$= \sum_{i,j=1}^{3} \frac{V_{N_{a,i+11}}^*(M_{N_1})_{i,j} V_{N_{j+8,b}}^T - V_{N_{a,i+8}}^*(M_{N_2}^{\dagger})_{i,j} V_{N_{j+3,b}}^T + V_{N_{a,i+5}}^*(M_{N_3})_{i,j} V_{N_{j+3,b}}^T}{v'},$$

$$(Y_R)^{ab} = -(Y_L^{\dagger})^{ab}, \qquad (III.30)$$

where we have used the following relations: $VV^{\dagger} = 1$ and $(\bar{\psi}_i \psi_j)^{\dagger} = -(\bar{\psi}_j \psi_i)$. Note that the GB interaction shown in Eq. (III.28) involves only the derivative couplings, which imply negligible contributions when coupled to vector currents.

2. The scalar boson φ_R

There are two relevant particles which may be of interests at colliders. The first one is the φ_R , which mixes with h_1 through the mixing angle α . We have mentioned the current limit on α is $\sin \alpha \lesssim 0.3$. Therefore, φ_R could be produced in exactly the same ways as the SM Higgs boson, namely, dominated by the gluon fusion (ggF) followed by vector-boson fusion, but suppressed by a factor $\sin^2 \alpha \lesssim 0.09$. For example, the ggF production rate for a φ_R of mass 500 GeV is approximately $5 \times 0.09 = 0.45$ pb. The decay modes for φ_R are similar to those of the SM Higgs boson, except that $\varphi_R \to H_1^0 H_1^0$ may now be possible and can be dominant. The size of this new channel depends on the $\lambda_{\varphi\Phi_1}$.

3. Drell-Yan production of $E'^+E'^-$

The second relevant signature is through the Drell-Yan production of the heavy charged fermion $E'_{L/R}$ of the doublet field $L'_{L/R}$. The E'^- so produced will decay into the neutral component of the doublet and the W boson (either real or virtual). The W boson can decay into a charged lepton and a neutrino for leptonic detection. The neutral component N' will decay into the SM neutrino(s) via mixing and the SM Higgs boson(s). One can detect the $b\bar{b}$ mode of the Higgs decay. Therefore, the final state of $E'^-E'^+$ production consists of two charged leptons and two $b\bar{b}$ pairs at Higgs boson mass plus missing energies.

IV. NUMERICAL ANALYSIS

Here we randomly select points for the input parameters within the following ranges for both the cases of NH and IH:

$$v_2 \in [0.1, 10] \text{ GeV}, m_D \in [10^{-10}, 10^{-4}], m \in [10^{-4}, 50] \text{ GeV},$$

 $m_{H^{\pm}} \in [500, 1000] \text{ GeV}, m_{h_2} \in [0.01, 10] \text{ GeV}, m_{A^0} \in [0.01, 100] \text{ GeV},$
 $[M_0, M_{N_1}, M_{N_2}, M_{N_3}, M_D, M, M', M_{L'}] \in [100, 1000] \text{ GeV},$ (IV.1)

where such a range of m_{h_2} is taken in order to compensate for the fermion-loop contribution of ΔS^f , whose typical value is 0.5. In the last line, the range stands for all the elements for each matrix. Note that $[M_{N_2}, M_{N_3}]$ are 3×2 matrices, M_0 is a 2×2 matrix, and $[M, M', M_{L'}]$ are 3×3 diagonal matrices, while we assume that $[m, m_D, M_D, M_{N_1}]$ are 3×3 symmetric matrices for simplicity.

We show scattered plots of θ_s^2 versus m_{ν_s} in Fig. 2 for NH and Fig. 3 for IH. The red points satisfy the constraint of ΔT . The allowed region ranges from $m_{\nu_s} \approx 0.5-50$ GeV with $\theta_s^2 \approx 10^{-12}-5 \times 10^{-10}$. The lifetime of ν_s should be shorter than 0.1 second that is equivalent to $\mathcal{O}(10^{23})$ GeV⁻¹. Notice here that, in addition to the usual modes such as $\nu_s \to \ell W/\nu_L Z$ that appear in the canonical seesaw scenario [24], we also have the mode $\nu_s \to \nu_L G$ via Y_L/Y_R , whose decay rate is given by $\frac{m_{\nu_s}}{4\pi} \sum_{i=1}^3 |\text{Im}(Y_L)^{4i}|^2$. Nevertheless, its lifetime is typically of the order 10^{-12} second which is shorter than the standard decay modes. Thus, the BBN bound can be negligible.

The upper region bounded by the orange line is covered in the FCC proposal, which gives the favored region of detecting the sterile neutrino in FCC. We notice that in the region around $m_{\nu_s} \approx 20 - 50$ GeV and $\theta_s^2 \approx 10^{-12} \sim 10^{-11}$, the parameter space of our model is indeed covered by the FCC proposal for both cases of NH and IH. It implies that our testability with the FCC experiment is more verifiable than the case of typical canonical seesaw model, although the detector's luminosity should be improved to some extent. This is the direct consequence of our huge matrix of the neutral fermions: 20×20 . Although the distribution of allowed region is similar between the NH and IH cases, the number of IH solutions are larger than NH. This is a natural consequence of the allowed range of neutrino oscillation data in Eq. (III.6) and Eq. (III.9).

⁷ In the typical canonical seesaw case, almost all of the region can be tested by the FCC experiment [24].

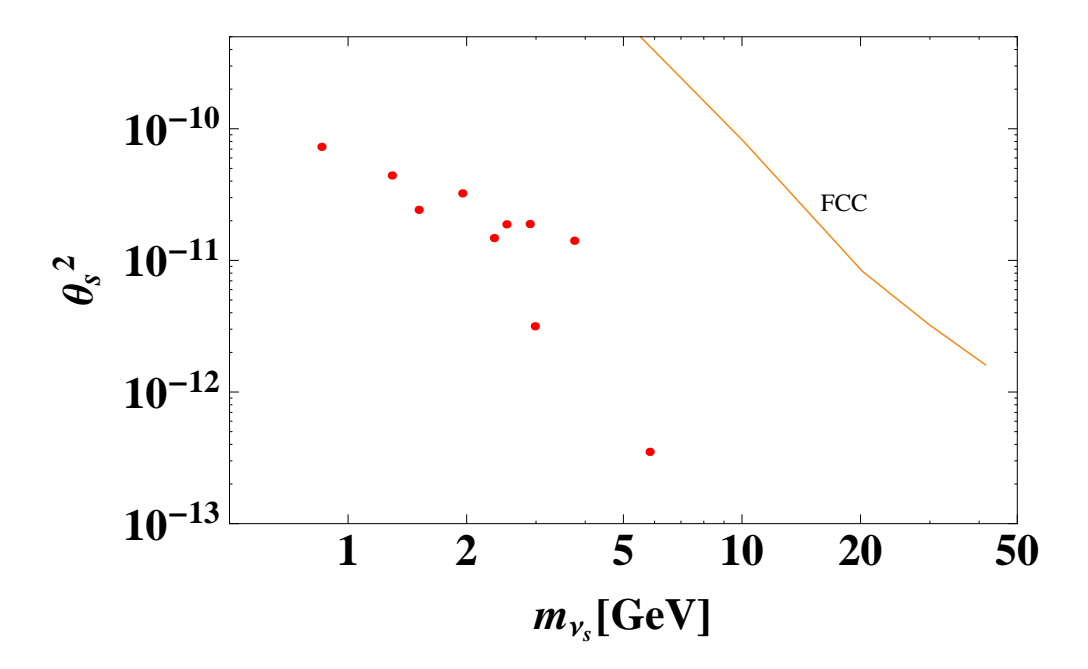


FIG. 2: Plots in terms of m_{ν_s} and θ_s in case of NH, where all the constraints discussed above are satisfied. The upper region bounded by the orange line is the favored region of detecting the sterile neutrino by FCC.

One might worry about the fact that we have no solution points that can simultaneously satisfy the ΔT constraint and be covered by the FCC experiment. Also, m_{h_2} may be too small to cause dangerous decays that violate our scenario. One of the simplest solutions is to introduce another boson in isospin doublet. For example, if we assign (2, 1/2, 1/2) under $(SU(2)_L, U(1)_Y, U(1)_L)$ for a new boson, we can obtain the measured ΔT without violating our discussion above and its neutral component can be a good dark matter candidate as an inert doublet boson. Its mass is at around 500 GeV to satisfy the relic density, which has already be discussed in Ref. [25].

V. CONCLUSIONS AND DISCUSSIONS

We have proposed a model with two neutrinophilic Higgs doublet fields $\Phi_{1,2}$, and the vacuum expectation value of the second Higgs doublet is only induced at one-loop level. As a result, the active neutrino masses can be naturally generated to be very small via the tiny VEV v_2 . We have also discussed various phenomenology or constraints from neutrino

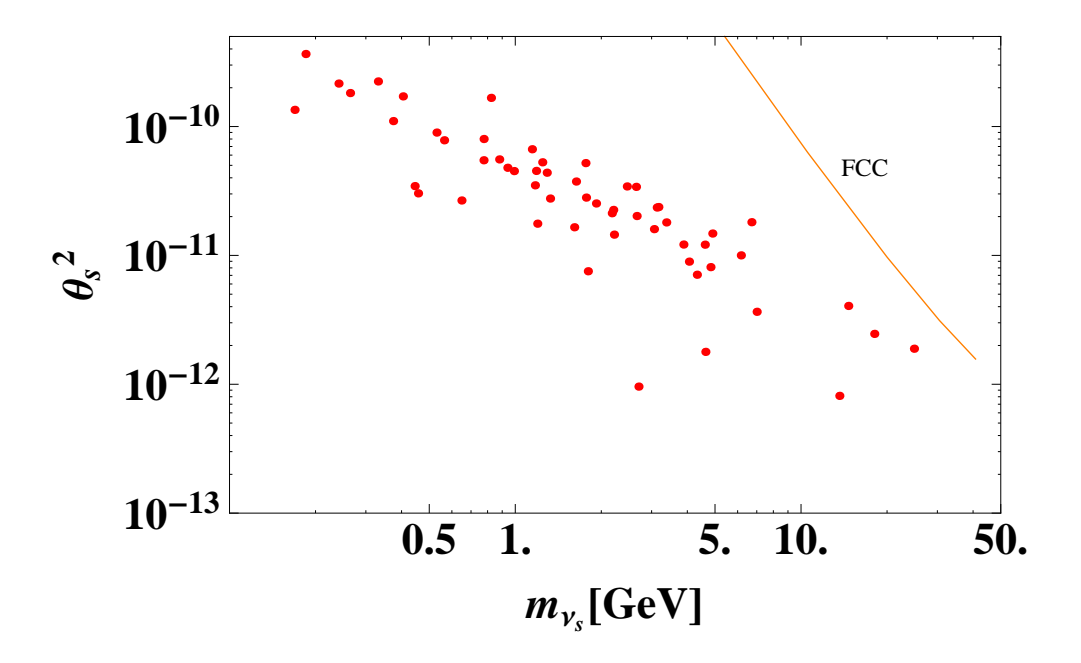


FIG. 3: Plots in terms of m_{ν_s} and θ_s in case of IH, where all the constraints discussed above are satisfied. The upper region bounded by the orange line is the favored region of detecting the sterile neutrino by FCC.

oscillation data, lepton-flavor violations, the oblique parameters and the muon g-2, and the possibilities of collider signatures. In addition, we have pointed out a possibility of sterile neutrino of mass O(0.1-10) GeV from the tiny VEV v_2 . Finally, we have shown a plot of m_{ν_s} and θ_s^2 that satisfy all the experimental bounds such as neutrino oscillation data, LFVs, and the oblique parameters. We have found an allowed region with $m_{\nu_s} \approx 20-50$ GeV and $\theta_s^2 \approx 10^{-12} \sim 10^{-11}$ that is covered by the proposal of the future FCC in pursuing the sterile neutrinos. It is one of the main results that our testability with the FCC experiment is more verifiable than the case of typical canonical seesaw model. This is the direct consequence of our huge matrix of the neutral fermions: 20×20 . For the muon g-2 we have obtained negative contributions that seem to be against the experimental fact. We may be able to detect a signature by looking at the decay of φ_R or by the Drell-Yan process of $E'^+E'^-$ at the LHC.

At the end of the discussion, it is worthwhile to mention a new possibility of detecting the Goldstone boson G. According to a recent work [26], G can be directly tested by the first order phase transitions in the early Universe triggered by discovery of gravitational waves at

the experiment of LIGO [27]. All of the valid terms to explain it are involved in our theory, our G can also be tested near future.

Acknowledgments

K.C. was supported by the MoST of Taiwan under Grant No. MOST-105-2112-M-007-028-MY3. H. O. is sincerely grateful for all the KIAS members in my stay.

Appendix A: Feynman Integrals

Definitions of $F(n, \alpha, \{A_i; n\})$ is the followings:

$$F(n,\alpha,\{A_i;n\}) \equiv \begin{cases} \int_0^1 \prod_{i=1}^n dx_i \delta(1-\sum_{i=1}^n x_i) \frac{1}{\left(\sum_{i=1}^n x_i A_i\right)^{\alpha}}. & (\alpha > 0) \\ \int_0^1 \prod_{i=1}^n dx_i \delta(1-\sum_{i=1}^n x_i) \log\left(\sum_{i=1}^n x_i A_i\right). & (\alpha = 0) \\ \int_0^1 \prod_{i=1}^n dx_i \delta(1-\sum_{i=1}^n x_i) \left(\sum_{i=1}^n x_i A_i\right)^{-\alpha} \left(\log\left(\sum_{i=1}^n x_i A_i\right) - \sum_{i=1}^{-\alpha} \frac{1}{i}\right). & (\alpha < 0) \end{cases}$$

Where $\{A_i; n\} = \{A_1, A_2, \dots, A_n\}$. The functions have following recurrence relations:

$$F(n,\alpha,\{A_i;n\}) = \frac{C_{\alpha}}{(A_{n-1} - A_n)} \times (F(n-1,\alpha-1,\{A_i;n-2,A_{n-1}\}) - F(n-1,\alpha-1,\{A_i;n-2,A_n\})),$$
(A.1)

where $\{A_i; n-2, B\} = \{A_1, A_2, \cdots, A_{n-2}, B\}$ and

$$C_{\alpha} = \begin{cases} \frac{1}{1-\alpha}. & (\alpha \neq 1) \\ 1. & (\alpha = 1) \end{cases}$$

We can obtain the formula of $F(n, \alpha, \{A_i; n\})$ using the recurrence relations and following relations:

$$F(1,\alpha,\{A;1\}) = \begin{cases} \frac{1}{A^{\alpha}}. & (\alpha > 0) \\ \log(A). & (\alpha = 0) \\ A^{-\alpha} \left(\log A - \sum_{i=1}^{-\alpha} \frac{1}{i}\right). & (\alpha < 0) \end{cases}$$

- [1] J. F. Gunion, H. E. Haber, G. L. Kane and S. Dawson, "The Higgs Hunter's Guide," Front. Phys. 80, 1 (2000).
- [2] S. Kanemura, T. Matsui and H. Sugiyama, Phys. Lett. B 727, 151 (2013) [arXiv:1305.4521 [hep-ph]].
- [3] T. Nomura and H. Okada, arXiv:1704.03382 [hep-ph].
- [4] W. Wang and Z. L. Han, Phys. Rev. D **94**, no. 5, 053015 (2016) doi:10.1103/PhysRevD.94.053015 [arXiv:1605.00239 [hep-ph]].
- [5] S. Kanemura and H. Sugiyama, Phys. Rev. D 86, 073006 (2012)doi:10.1103/PhysRevD.86.073006 [arXiv:1202.5231 [hep-ph]].
- [6] H. Okada and Y. Orikasa, Phys. Rev. D 93, no. 1, 013008 (2016) doi:10.1103/PhysRevD.93.013008 [arXiv:1509.04068 [hep-ph]].
- [7] K. Cheung, H. Ishida and H. Okada, arXiv:1609.06231 [hep-ph].
- [8] N. R. Agostinho, G. C. Branco, P. M. F. Pereira, M. N. Rebelo and J. I. Silva-Marcos, arXiv:1711.06229 [hep-ph].
- [9] E. Fernandez-Martinez, J. Hernandez-Garcia and J. Lopez-Pavon, JHEP 1608, 033 (2016)doi:10.1007/JHEP08(2016)033 [arXiv:1605.08774 [hep-ph]].
- [10] D. V. Forero, M. Tortola and J. W. F. Valle, Phys. Rev. D 90, no. 9, 093006 (2014) doi:10.1103/PhysRevD.90.093006 [arXiv:1405.7540 [hep-ph]].
- [11] A. M. Baldini *et al.* [MEG Collaboration], Eur. Phys. J. C **76**, no. 8, 434 (2016) [arXiv:1605.05081 [hep-ex]].
- [12] J. Adam et al. [MEG Collaboration], Phys. Rev. Lett. 110, 201801 (2013) [arXiv:1303.0754 [hep-ex]].
- [13] K. A. Olive et al. [Particle Data Group], Chin. Phys. C 38, 090001 (2014).
- [14] R. Barbieri, L. J. Hall and V. S. Rychkov, Phys. Rev. D 74, 015007 (2006) doi:10.1103/PhysRevD.74.015007 [hep-ph/0603188].
- [15] C. Patrignani *et al.* [Particle Data Group], Chin. Phys. C 40, no. 10, 100001 (2016). doi:10.1088/1674-1137/40/10/100001
- [16] K. Nishiwaki, H. Okada and Y. Orikasa, Phys. Rev. D 92, no. 9, 093013 (2015) doi:10.1103/PhysRevD.92.093013 [arXiv:1507.02412 [hep-ph]].

- [17] H. Hatanaka, K. Nishiwaki, H. Okada and Y. Orikasa, Nucl. Phys. B 894, 268 (2015) doi:10.1016/j.nuclphysb.2015.03.006 [arXiv:1412.8664 [hep-ph]].
- [18] K. Cheung, W. Y. Keung and T. C. Yuan, Phys. Rev. D 89, no. 1, 015007 (2014) doi:10.1103/PhysRevD.89.015007 [arXiv:1308.4235 [hep-ph]].
- [19] E. K. Akhmedov, Z. G. Berezhiani, R. N. Mohapatra and G. Senjanovic, Phys. Lett. B 299, 90 (1993) doi:10.1016/0370-2693(93)90887-N [hep-ph/9209285].
- [20] S. Weinberg, Phys. Rev. Lett. 110, no. 24, 241301 (2013) doi:10.1103/PhysRevLett.110.241301[arXiv:1305.1971 [astro-ph.CO]].
- [21] A. Latosinski, K. A. Meissner and H. Nicolai, arXiv:1205.5887 [hep-ph].
- [22] A. Blondel et al. [FCC-ee study Team], Nucl. Part. Phys. Proc. 273-275, 1883 (2016) doi:10.1016/j.nuclphysbps.2015.09.304 [arXiv:1411.5230 [hep-ex]].
- [23] S. Alekhin et al., Rept. Prog. Phys. 79, no. 12, 124201 (2016) doi:10.1088/0034-4885/79/12/124201 [arXiv:1504.04855 [hep-ph]].
- [24] R. W. Rasmussen and W. Winter, Phys. Rev. D 94, no. 7, 073004 (2016) doi:10.1103/PhysRevD.94.073004 [arXiv:1607.07880 [hep-ph]].
- [25] T. Hambye, F.-S. Ling, L. Lopez Honorez and J. Rocher, JHEP 0907, 090 (2009) Erratum: [JHEP 1005, 066 (2010)] doi:10.1007/JHEP05(2010)066, 10.1088/1126-6708/2009/07/090 [arXiv:0903.4010 [hep-ph]].
- [26] A. Addazi and A. Marciano, arXiv:1705.08346 [hep-ph].
- [27] C. Caprini et al., JCAP 1604, no. 04, 001 (2016) doi:10.1088/1475-7516/2016/04/001 [arXiv:1512.06239 [astro-ph.CO]].